Hydrothermal treatment and Mesoporosity of MCM-41 mesoporous nanocomposite

Nasir Vadia, Diti Desai and Sadhana Rajput
Pharmacy Department, M. S. University of Baroda, Centre of Relevance and Excellence in New Drug Delivery System, Vadodara 390002, Gujarat. India.

ARTICLE INFO

ABSTRACT

Considerable research efforts have been made in recent years towards the development of silica mesoporous nanocomposite as drug delivery system. Numerous reports are available in literature for the synthesis of mesoporous nano materials. In present work two distinct mesoporous MCM-41 nanocomposite (MCM-41-A and MCM-41-B) were synthesized and characterized by different instrumental techniques such as X-ray diffraction, scanning electron microscopy, transmission electron microscopy, FTIR and nitrogen adsorption desorption analyses. Both the mesoporous nanocomposite was synthesized with different hydrothermal treatment and effect on mesoporosity was determined. Evaluation data revealed MCM-41-A MSNs with regular spherical shape with high degree of mesoporosity whereas MCM-41-B MSNs were lack of mesoporous characteristics. For instance, hydrothermal treatment significantly affects the physical properties like surface area, pore volume and pore diameter of the MSNs.

INTRODUCTION

Mesoporous silica attracted a lot of interest in recent years since their introduction by researchers of Mobil Oil Company in 1992. The family of highly ordered mesoporous nanocomposite, designated as M41S have been used as immobilization supports for enzymes and proteins, in membranes, sensors, and in biological applications (Beck *et al.,* 1992; Blin *et al.,* 2000). Mesoporous materials have been reported to be used in sequestering nuclear waste and heavy metals, as hosts for luminescent materials for laser and optical device applications (Xu *et al.,* 2003). The feasibility of modification and rich morphology of these nanocomposite make them the promising tool for various fields from material science to medical science (Corma *et al.,* 1994). Different synthesis methodology are developed and reported by various research groups according to the required applications (Sierra *et al.,* 2000). Mesoporous MCM-41 nanocomposite (MSN) is generally characterized by hexagonal arrangement of uniform mesopores with tunable pore sizes, high

surface area and high pore volume. The synthesis of MSNs includes the use of inorganic silica and surfactant as structure directing agents. The formation of mesoporous structure owing to interaction between the negatively charged silicate species and the positive charged surfactant micelles (Ciesla *et al.,* 1999). The surfactant is removed either by calcination or solvent extraction procedure; leaving the porous silicate network. The well defined inner structure consists of unidirectional channel like pores and is well arranged in hexagonal pattern. Moreover, the pore wall contains surface silanol groups (Bruhwiler *et al.,* 2004).

The mesoporous characteristics of the materials make them suitable for hosting and further delivering of a variety of chemical and biological molecules. The mesoporosity of nanocomposite can be controlled by a sophisticated choice of surfactants and auxiliary organic chemicals. It was found that the pore diameter of MSNs can be controlled through the carbon chain length of the surfactant used during synthesis (Kruk et al, i1997, Horcajada *et al.,* 2004, Letellier *et al.,* 2006). Some auxiliary compound like 1, 3, 5-trimethyl benzene and triisopropyl benzene are effectively used to enlarge the size of micelles leading to pore enlargement (Beck *et al.,* 1992, Kimura *et al.,* 1992).

* Corresponding Author
"NIMMAT", Plot no. 549, A/3, Sir Pattani road, Opp. Gujarat travels
main office, Crescent, Bhavnagar- 364 001
Mobile No: 09879858144

Addition of alkanes such as n-pentane, n-hexane, n-heptane, n-octane and n-dodecane and N, N-dimethyl hexadecylamine during the synthesis can interact with the micelles of cationic surfactants, leads to the mesopore enlargement (Blin *et al.,* 2000). The hydrothermal treatment at specific temperature and time is another method of obtaining stable and enlarged mesopores (Huo *et al.,* 1996, Sayar *et al.,* 1997., Mokaya *et al.,* 1999). The low-temperature usually results in imperfect silica condensation of mesoporous materials with a large amount of terminal OH group which make the mesostructure unstable (Corma et al, i1997).

In general, MSNs, if developed at elevated temperature, has positive influence on the structural characteristics. Synthesis at elevated temperature will increase the nucleation rate and their linear growth rate. Thus change in synthesis condition, especially aging time greatly affects the mesoporosity of the MCM-41.

In present study, MCM-41 MSNs were synthesized with varied hydrothermal time and change in their mesoporosity was determined. The result of the study revealed that the continuous hydrothermal treatment is important for the development of mesoporosity of MSNs. It was observed that the hydrothermal treatment provided with three consecutive cycles (each, 8 h) lead to formation of irregular shaped particles with lack of mesoporous structure. The synthesized MCM-41 MSNs were characterized by scanning electron microscopy, transmission electron microscopy, X-ray powder diffraction, differential scanning calorimetry, FT-IR spectroscopy, Brunauer Emmett and Teller (B.E.T.) specific surface area and pore volume.

EXPERIMENTAL

Materials

Tetraethyl orthosilicate (TEOS), cetyltrimethyl ammonium bromide (CTAB), tetra methyl ammonium hydroxide (TMAOH), and fumed silica were obtained from Sigma Aldrich (USA). Double distilled water was used throughout the study. Other reagents and solvents were of reagent grade and were used without further purification.

Synthesis of mesoporous MCM-41

MCM-41 silica-based mesoporous material was synthesized using the following procedure (Ghiaci *et al.,* 2004). Accurately weighed 9.84 g of CTAB was dissolved in 67 g of deionized water. It was then stirred on a magnetic stirrer for 5 min. Then 6.92 g TMAOH was added drop wise to it with constant stirring. The mixture was stirred for 10 min and silica source, fumed silica (6 g) was added to the solution under stirring. The vigorous stirring was further continued for 1.5 h. The resulting gel of composition SiO_2:0.27 CTAB: 0.19 TMAOH: 40 H_2O was heated in a sealed stainless steel autoclave at 383K for hydrothermal treatment.

Hydrothermal treatment was conducted in teflon lined stainless steel autoclave. For the MCM-41-A, continuous 24 h of hydrothermal treatment was provided whereas for MCM-41-B, instead of continuous 24 h, three cycles each of 8 h per day was

used. The products were recovered by filtration, washed thoroughly with distilled water and then dried at 313K for 4 h. Surfactant was removed by ignition process in the muffle furnace, heated at 823K, under air flow for 5 h.

Characterization of synthesized MCM-41

The morphology of synthesized MCM-41-A and MCM-41-B mesoporous nanocomposite were examined by scanning electron microscopy (SEM) operated at an acceleration voltage of 10 kV. The samples were attached to aluminum stubs with double side adhesive carbon tape then gold coated and examined using a scanning electron microscope (Leo 1430 VP-Germany). A high resolution electron microscopy image of the mesoporous MCM-41-A and MCM-41-B mesoporous nanocomposite were taken with a JEOL JEM-2100 electron microscope (USA), equipped with a pole piece, operated at 120 kV. The powder samples were grounded softly in a mortar and dispersed in ethanol in an ultrasonic bath for several minutes. A few drops were then deposited on 200 mesh copper grids covered with a holey carbon film. The electron micrographs were recorded in electron negative films and in a digital PC system attached to the electron microscope. Differential scanning calorimetry (Shimadzu DSC-60- Japan) analyses were performed using an automatic thermal analyser (Shimadzu TA 60- WS- Japan). Aluminum pans were employed in the experiments for all samples and an empty pan, prepared in the same manner, was used as a reference. Samples of 3 mg were weighted directly into the aluminum pan which was firmly crimped around the lid to provide an adequate seal. The thermal analyses were conducted from ambient temperature to 300^0C at a pre-programmed heating rate of 10^0C per min.

FT-IR spectra were recorded in air, at room temperature on a Bruker alpha-T (Germany). Samples were prepared by gently grounding the powders with KBr. The data region was 4000–900cm^{-1}. Mesoporous MCM-41-A and MCM-41-B mesoporous nanocomposite were evaluated using an X'Pert- MPD powder x-ray diffraction (Philips- Netherland). In all cases, the generator was operated at 40 kV and 30 mA. In order to avoid the problem of illuminated area at low 2u angles, all the samples were measured using the same sample holder. The mesoporous samples were scanned from 1 to 9 of diffraction angle (2θ) at scanning speed of 0.02 2θ/5s.

Nitrogen adsorption- desorption isotherms were determined using a computer controlled Micromeritics ASAP-2010 apparatus. Prior to adsorption measurements, both the MCM-41 mesoporous nanocomposite were degassed under vacuum over night at 423K overnight in the port of the adsorption analyzer. The specific surface area was determined by application of the B.E.T. method to the isotherm.

RESULTS AND DISCUSSION

The scanning electron microscopic images of the samples MCM-41-A and MCM-41-B are shown in fig.1. MCM-41-A samples exhibit regular sphere shaped particles having smooth

surface morphology. The micrographs taken by scanning electron microscope of MCM-41-B samples represent the loose aggregate and irregularly shaped particles (Fig. 2). The morphological characteristics of the both the mesoporous, i.e. MCM-41-A and MCM-41-B were evaluated by transmission electron microscope (Fig. 3 and Fig. 4). The micrographs taken by transmission electron microscope of MCM-41-A revealed a characteristic hexagonal honeycomb pattern (Fig. 3) whereas MCM-41-B sample is devoid of hexagonal characteristics with complete absence of mesopores in its structure (Fig. 4). Fig. 5 shows the X-ray diffraction patterns of MCM-41-A and MCM-41-B. MCM-41-A diffractogram showed typical reflections between 2° and 9° (Schulz-Ekloff et al, i1999). It can be seen that X-ray diffraction patterns of MCM-41-A presents a strong (100) diffraction peak with two small (110) and (200) diffraction peaks, confirming the formation of highly ordered 2D hexagonal mesostructures. On the other hand, X-ray diffraction patterns of MCM-41-B show the absence of the peaks as it observed in MCM-41-A, i.e. at 100, 110 and 200. This revealed that the MCM-41-B has no hexagonal characteristics and completely lack of mesoporosity.

In Fig. 6 nitrogen adsorption-desorption isotherms of MCM-41-A and MCM-41-B are presented. MCM-41-A shows typical type IV isotherm according to IUPAC classification indicating the mesoporosity of the material. The isotherm of MCM-41-A shows a hysteresis loop at high relative pressure, which has been ascribed to the presence of interparticle porosity (Brunauer et al, i1938, Choma *et al.,* 2002).

However, isotherm of MCM-41-B does not follow the typicality of type IV isotherm which is defined by IUPAC. The isotherm of MCM-41-B does not show the hysteresis loop indicating the absence of mesoporosity of the material.

The calculated BET specific surface area for MCM-41-A and MCM-41-B were 739 and 115 m²/g, respectively. The data obtained from BET surface area revealed that MCM-41-B was not fulfilling the characteristics of mesoporous MCM-41 type nanocomposite.

Fig. 7 represents the FTIR spectrum of both the mesoporous nanocomposite. Spectrum of MCM-41-A showed the presence of a vibration band at 3740 cm^{-1} attributable to isolated terminal silanol groups and of another large band at 3611 cm^{-1} attributable to geminal and associated terminal silanol groups. The stretching vibrations of Si-O-Si and Si-OH can be seen at 1070 and 958 cm^{-1}.

FTIR spectrum of MCM-41-B showed the absence of all the peaks as it observed in MCM-41-A, i.e. at 3740 cm^{-1} for isolated terminal silanol groups, 3611 cm^{-1} for geminal and associated terminal silanol groups and absence of stretching vibration at 1070 cm^{-1} and 958 cm^{-1}.

Fig. 8 shows differential scanning calorimetric thermograms of MCM-41-A and MCM-41-B. The DSC curve of MCM-41-A exhibits a straight line, corresponding to its intrinsic thermal stability. MCM-41-B indicates the straight line followed by slope. That can be due to absence of phase transitions and mesoporosity.
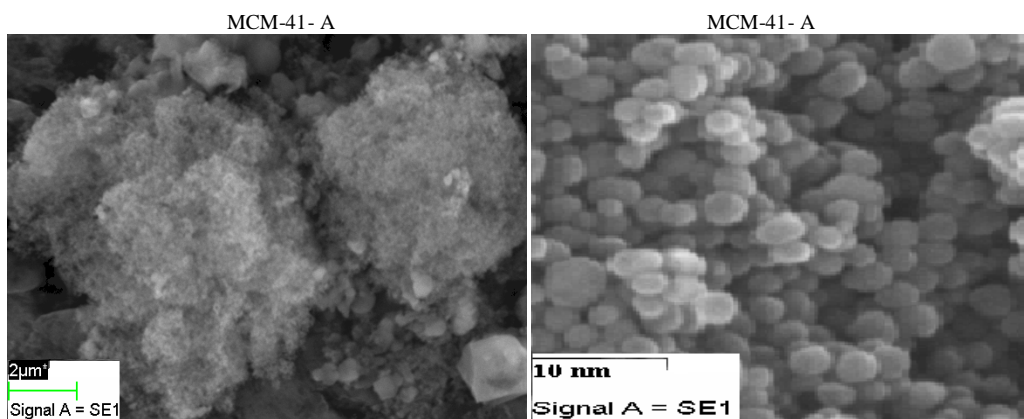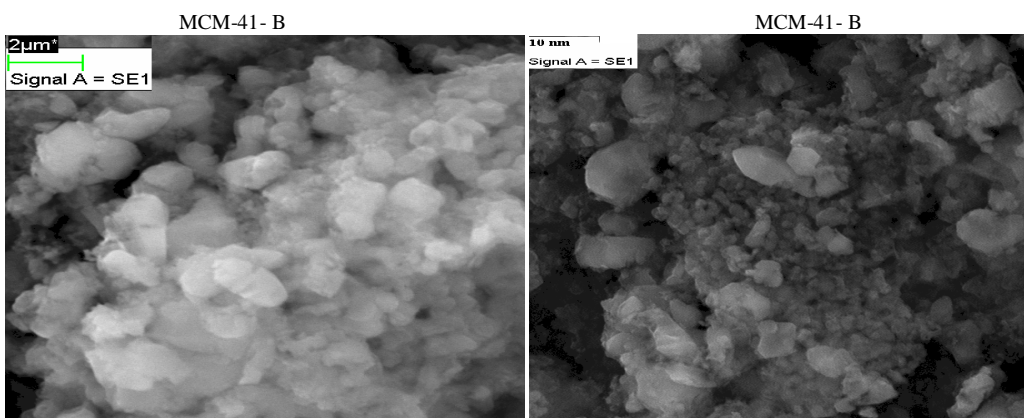

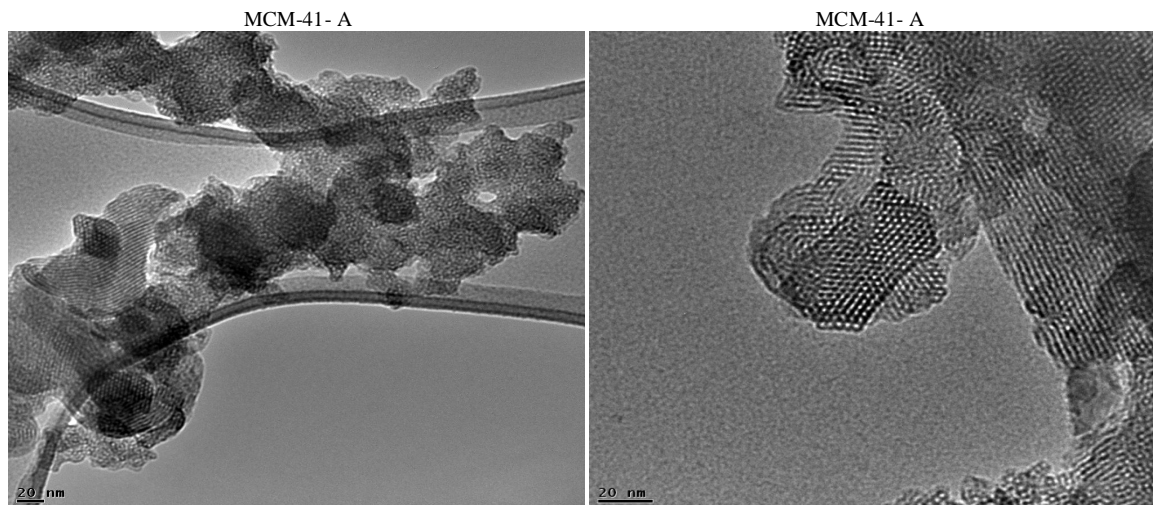**Fig. 1:** SEM images of MCM-41-A.

Fig. 2: SEM images of MCM-41-B

MCM-41- A   MCM-41- A

Fig. 3: TEM images of MCM-41-A.
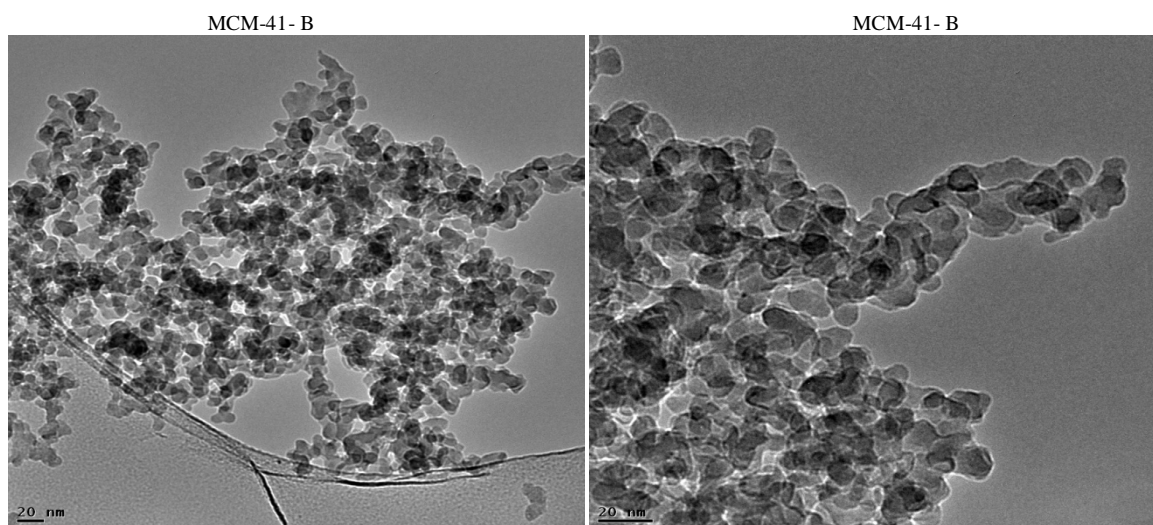
MCM-41- B   MCM-41- B

Fig. 4: TEM images of MCM-41-B
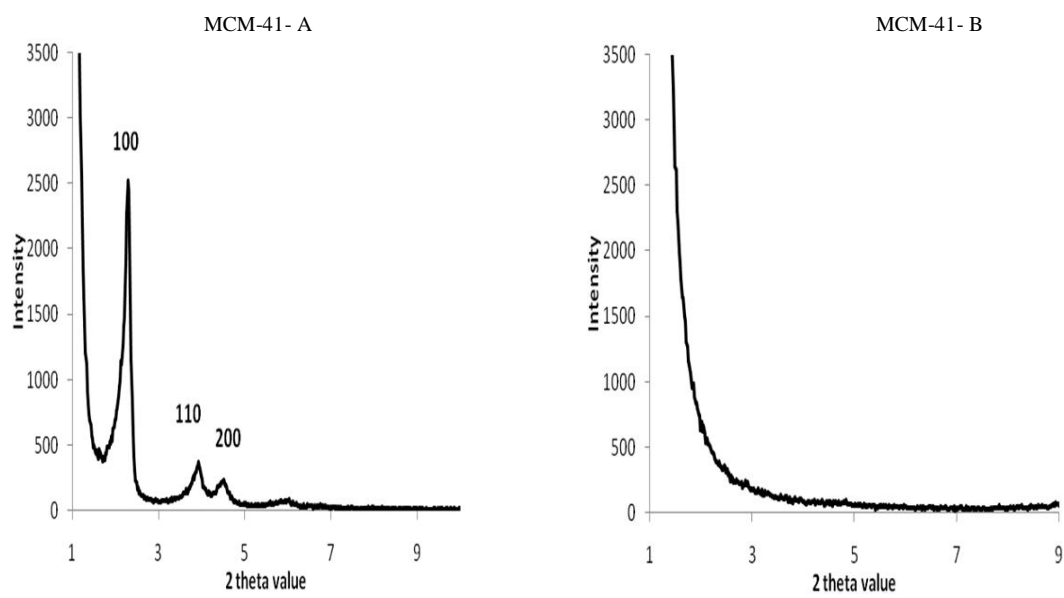
MCM-41- A   MCM-41- B

Fig. 5: XRD pattern of MCM-41-A and MCM-41-B
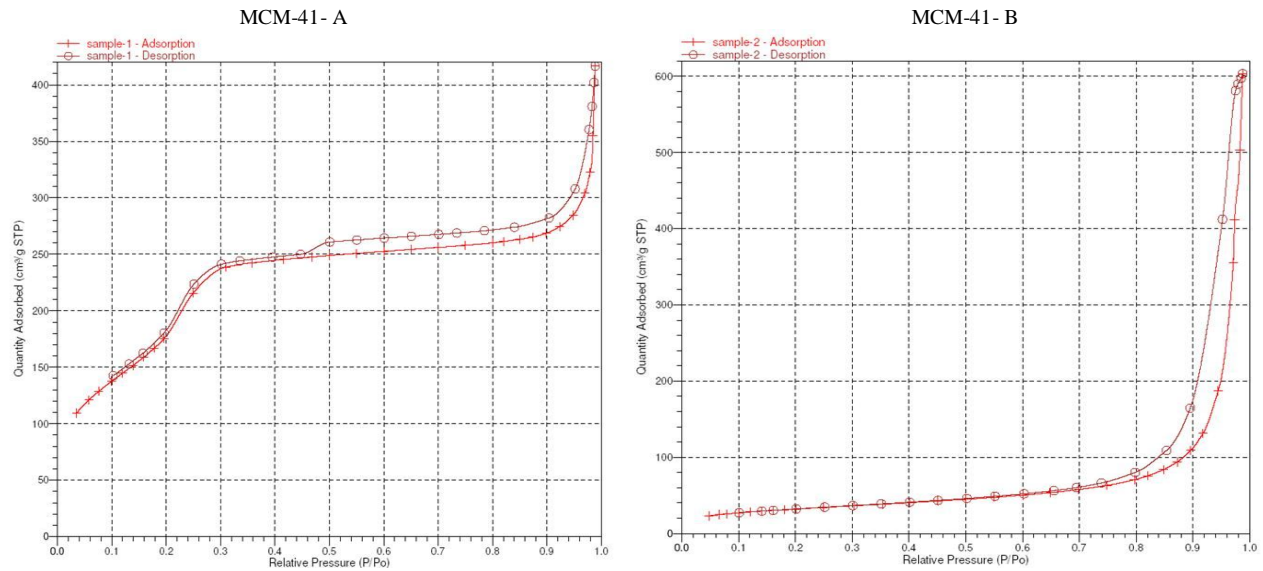
MCM-41- A   MCM-41- B

Fig. 6: N_2 adsorption–desorption isotherms of MCM-41-A and MCM-41-B

MCM-41- A

MCM-41- B

Fig. 7: FTIR spectrum of MCM-41-A and MCM-41-B
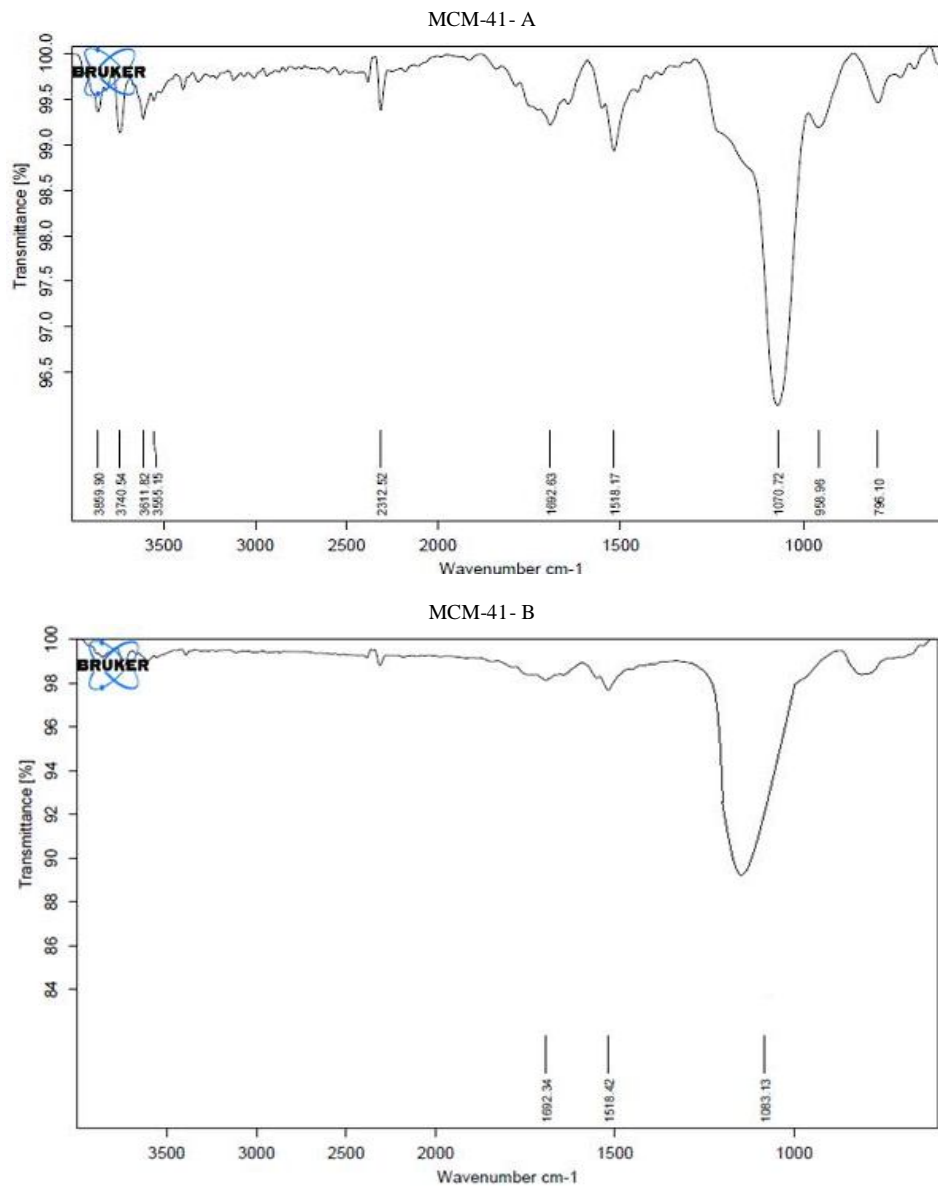
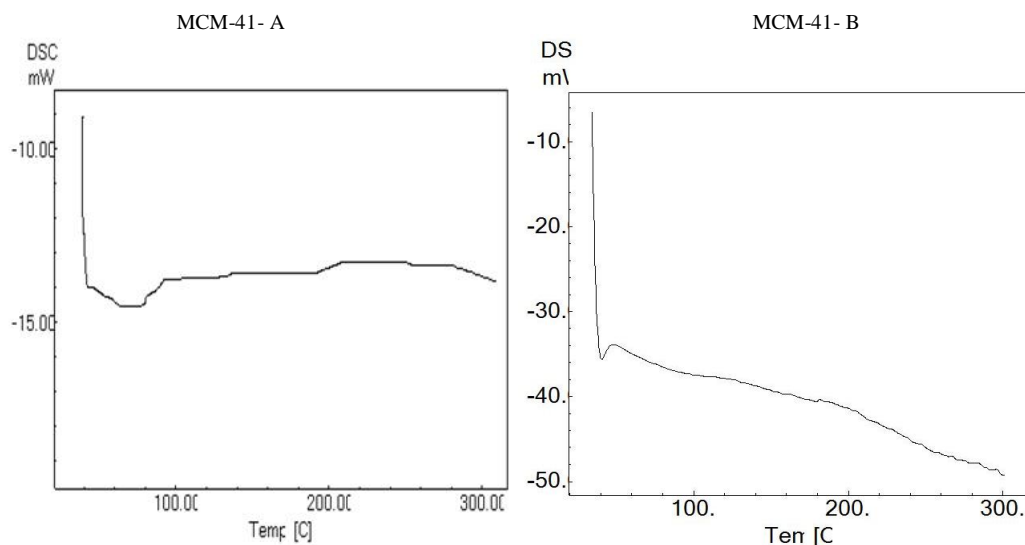MCM-41- A   MCM-41- B

Fig. 8: DSC thermogram of MCM-41-A and MCM-41-B

CONCLUSION

The current study demonstrated that apart from different synthesis factors, change in hydrothermal time greatly affects the structural characteristics of MCM-41 mesoporous nanocomposite. The interrupted hydrothermal treatment results in drastic change of mesoporosity. For the development of mesoporous MCM-41 nanocomposite with well defined mesostructure, it is very important to provide proper hydrothermal treatment proper selection of temperature and time.

REFERENCES

Beck JS, Vertuli JC, Roth WJ, Leonowicz ME, Kresge CT, Schmitt KD, Chu C, Olson DH, Sheppard EW, McCullen SB, Higgins JB and Schlenker JL. A new family of mesoporous molecular sieves prepared with liquid crystal templates. J Am Chem Soc. 1992; 114: 10834-43.

Blin JL, Otjacques C, Herrier G and Su BL. Pore size engineering of mesoporous silicas using alkanes as swelling agents. Stud Surf Sci Catal. 2000; 129: 75-84.

Bru¨hwiler D and Calzaferri G. Molecular sieves as host materials for supramolecular organization. Micropor Mesopor Mater. 2004; 72: 1–23.

Brunauer S, Emmet P and Teller E. Adsorption of gases in multi molecular layers. J Am Chem Soc. 1938; 60: 309–19.

Choma J, Jaroniec M, Burakiewicz-Mortka W and Kloske M. Critical appraisal of classical methods for determination of mesopore size distributions of MCM-41 materials. Appl Surf Sci. 2002; 196: 216–23.

Ciesla U and Schu,¨th F. Ordered mesoporous materials. Micropor Mesopor Mater. 1999; 27: 131-49.

Corma A, Fornes V, Navarro MT and Pe´rez-Patiente J. Acidity and stability of MCM-41 crystalline aluminosilicates. J Catal. 1994; 148: 569–74.

Corma A. From microporous to mesoporous molecular sieve materials and their use in catalysis. Chem Rev. 1997; 97: 2373-2420.

Diaz JF and Balkus KJ. Enzyme immobilization in MCM-41 molecular sieve. J Mol Catal B: Enzym. 1996; 2: 115-26.

Ghiaci M, Abbaspur A, Kia R and Seyedeyn-Azad F. Equilibrium isotherm studies for the sorption of benzene, toluene, and phenol onto organo-zeolites and as-synthesized MCM-41. Sep Purif Technol. 2004; 40: 217–29.

Horcajada P, Ramila A, Perez-Pariente J and Vallet-Regi M. Influence of pore size of MCM-41 matrices on drug delivery rate. Micropor Mesopor Mater. 2004; 68: 105- 9.

Huo Q, Margolez DI and Stucky GD. Surfactant control of phases in the synthesis of mesoporous silica-based materials. Chem Mater. 1996; 8: 1147-60.

Kimura T, Sugahara Y and Kuroda K. Synthesis and characterization of lamellar and hexagonal mesostructured aluminophosphates using alkyl trimethyl ammonium cations as structure directing agents. Chem Mater. 1992; 11: 508-18.

Kruk M, Jaroniec M and Sayari A. Adsorption study of surface and structural properties of MCM-41 materials of different pore sizes. J Phy Chem B. 1997; 110: 583-89.

Letellier FJ, Blanchard K, Fajerwerg C, Louis M, Breysse D and Guillaume D (). Search for confinement effects in mesoporous supports: hydrogenation of o-xyleneon Pt degrees/MCM-41. Catal Lett. 2006; 110: 115-24.

Mokaya R. Improving the stability of mesoporous MCM-41 silica via thicker more highly condensed pore walls. J Phys Chem B. 1999; 103: 10204-08.

Moller K and Bein KT. Inclusion chemistry in periodic mesoporous host. Chem. Mater. 1998; 10: 2950-63.

Sayar A, Liu P, Kruk M and Jaroniec M. Characterization of large-pore MCM-41 molecular sieves obtained via hydrothermal restructuring. Chem Mater. 1997; 9: 2499-2506.

Schulz-Ekloff G, Rathousky J and Zukal A. Controlling of morphology and characterization of pore structure of ordered mesoporous silica. Micropor Mesopor Mater. 1999; 27: 273–85.

Sierra L, Lopez B and Guth JL. Mesoporous silica preparation of particles with controlled morphology from sodium silicate solutions and a non-ionic surfactant at pH values Between 2 and 6. Micropor Mesopor Mater. 2000; 39: 519–27.

Xu W, Luo Q, Wang H, Francesconi LC, Stark RE and Akins DL. A polyoxoanion occluded within modified MCM-41: spectroscopy and structure. J Phys Chem B. 2003; 107: 497–501.